


 Cite this: *RSC Adv.*, 2021, **11**, 13769

## Promotion effects of flavonoids on browning induced by enzymatic oxidation of tyrosinase: structure–activity relationship

 Yao Lu, <sup>a</sup> Yi Xu, <sup>a</sup> Meng-Ting Song, <sup>a</sup> Ling-Ling Qian, <sup>a</sup> Xiao-Lin Liu, <sup>a</sup> Rong-Yao Gao, <sup>a</sup> Rui-Min Han, <sup>a\*</sup> Leif H. Skibsted <sup>b</sup> and Jian-Ping Zhang <sup>a</sup>

Tyrosinase, widely distributed in nature, is a copper-containing polyphenol oxidase involved in the formation of melanin. Flavonoids are most often considered as tyrosinase inhibitors but have also been confirmed to be tyrosinase substrates. Four structure-related flavonoids including flavones (apigenin and luteolin) and flavonols (kaempferol and quercetin) are found to promote not inhibit browning induced by tyrosinase catalyzed oxidation both in model systems and in mushrooms under aerobic conditions. A comparison with enzymatic oxidation and autoxidation of flavonoids alone has helped to clarify why flavonoids function as a substrate rather than an inhibitor. Flavonoids almost do not affect the kinetics of melanin formation from enzymatic oxidation of L-dopa in excess. In addition, a new brown complex formed during the reaction of flavonoid quinone and dopaquinone is suggested to enhance the browning effects by competing with isomerization and autoxidation. Structure–activity relationships of the four flavonoids in melanin formation leading to browning induced by autoxidation and enzymatic oxidation confirm the enzymatic nature of the browning.

Received 19th February 2021

Accepted 5th April 2021

DOI: 10.1039/d1ra01369f

rsc.li/rsc-advances

### Introduction

Tyrosinase (TYR) is a crucial enzyme in melanin biosynthesis in animals, bacteria, plants, and fungi.<sup>1</sup> Tyrosinase has been recognized to catalyze tyrosine monophenol and synthesize intermediates including L-dopa o-diphenol, dopaquinone, cyclodopa and dopachrome (DC), which further polymerizes to form brown or black melanin pigments.<sup>2–6</sup> In animals, melanin can protect the skin from ultraviolet radiation damage. However, excessive production of melanin causes freckles, melasma, age spots, and under some conditions may induce skin cancer.<sup>7</sup> In vegetables and fruits, tyrosinase also catalyzes the oxidation of bioactive constituents of fruit and vegetables, which leads to unfavorable enzymatic browning, damage of nutrients and sensory properties.<sup>8</sup>

Tyrosinase inhibitors have attracted great attention in relation to medical, cosmetic and food products due to their preventive effects in pigmentation disorders, skin aging and food browning. Hydroquinone, kojic acid, corticosteroid and arbutin have been known to be efficient tyrosinase inhibitors, but their serious side effects such as permanent

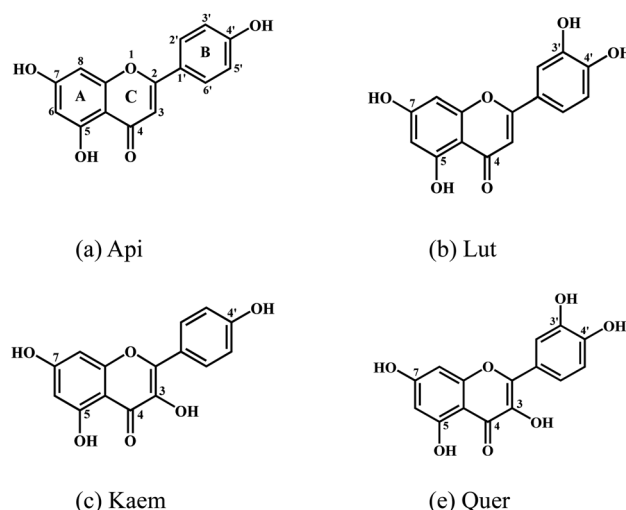
depigmentation, erythema, contact dermatitis, and skin cancer among others, limit their applications.<sup>9–12</sup> Flavonoids, as natural antioxidants abundant in fruits and vegetables as well as components in traditional herbal medicine,<sup>13</sup> have been identified, based on kinetic studies in model systems, as tyrosinase inhibitors inhibiting formation of the intermediate DC absorbing at 475 nm during oxidation of L-dopa as substrate.<sup>14–19</sup> Some flavonoids have even been characterized as strong tyrosinase inhibitors.<sup>20–26</sup> However, interference of flavonoids reacting with o-quinone was recently found to inhibit the enzymatic reactions and therefore to complicate determination of tyrosinase activity in the presence of flavonoids.<sup>27</sup> The effects of flavonoids serving as both inhibitors and substrates of tyrosinase on melanin formation and browning are accordingly still not clear.

In this kinetic study, spectroscopic methods were employed to reveal the effects of four structure-related flavonoids on melanin formation and browning induced by enzymic oxidation of tyrosinase both in model system with L-dopa oxidation and in browning of mushrooms as a food example. Except for two 5,7-phenols in ring A, apigenin (Api) contains one 4'-phenolic groups in ring B, and luteolin (Lut) has an additional 3'-phenol compared with Api. Kaempferol (Kaem) and quercetin (Quer) have an additional 3-phenol in ring C compared with Api and Lut, respectively, as shown in Scheme 1. Mushroom tyrosinase (EC 1.14.18.1), as the only commercially available tyrosinase, was used in model system due to its highest homology with mammalian tyrosinase among different tyrosinases.<sup>28,29</sup> The browning of mushroom has been confirmed to be the enzymatic

<sup>a</sup>Department of Chemistry, Renmin University of China, Beijing, 100872, China  
 E-mail: rmhan@ruc.edu.cn; yaolu102294@ruc.edu.cn; mtsong2019@ruc.edu.cn; qianlingling@ruc.edu.cn; liuxl2018@ruc.edu.cn; rygao@ruc.edu.cn; jpzhang@ruc.edu.cn; Fax: +86-10-6251-6444; Tel: +86-10-6251-6604

<sup>b</sup>Department of Food Science, University of Copenhagen, Rolighedsvej 30, DK-1958 Frederiksberg C, Denmark. E-mail: ls@food.ku.dk





**Scheme 1** Molecular structures of (a) apigenin, Api, (b) luteolin, Lut, (c) kaempferol, Kaem and (d) quercetin, Quer.

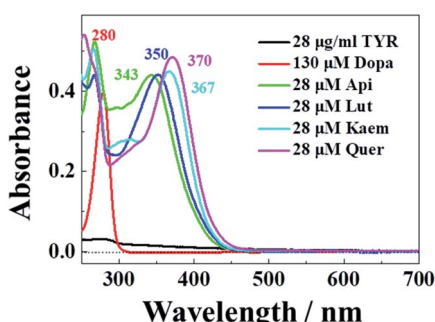


**Fig. 1** Absorption spectra of  $28 \mu\text{g mL}^{-1}$  tyrosinase,  $130 \mu\text{M}$  L-dopa and  $28 \mu\text{M}$  Api, Lut, Kaem, and Quer, respectively.

oxidation of amino acid tyrosine by tyrosinase.<sup>30</sup> *Agaricus bisporus*, also known as white mushroom, containing a variety of amino acids, nucleotides and vitamins,<sup>31–33</sup> was used for comparison with the model systems studied.

## Results

To elucidate effects of flavonoids on melanin formation and browning induced by tyrosinase, enzymatic oxidation of L-dopa pre-incubated with flavonoids by tyrosinase in ternary system and of flavonoids by tyrosinase in binary system as well as autoxidation of flavonoids alone were investigated in comparison in air-saturated aqueous solution by the use of time-dependent absorption spectra. The changes of white mushroom in color were recorded to investigate the effect of flavonoids on browning of food system by using diffuse reflection spectra. Since the enzymatic oxidation of flavonoids by tyrosinase occurs on a slower minute timescale compared with the rate of flavonoids binding with tyrosinase as seen below in Fluorescence of tyrosinase quenched by flavonoids section, fluorescence spectroscopy was applied to study the interaction of flavonoids with tyrosinase in aqueous solution.

### Interaction of flavonoids with tyrosinase

The characteristic absorption of tyrosinase, L-dopa and individual flavonoids, Api, Lut, Kaem and Quer at 250–350 nm were shown in Fig. 1. At the excitation wavelength of 280 nm, the fluorescence emission spectra of tyrosinase with different concentrations of flavonoids were collected, as shown in Fig. 2a–d. Fluorescence spectra were calibrated to eliminate the inner filter and reabsorption of flavonoids according to eqn (1)<sup>34,35</sup>

$$F = F_m \times e^{(A_1 + A_2)/2} \quad (1)$$

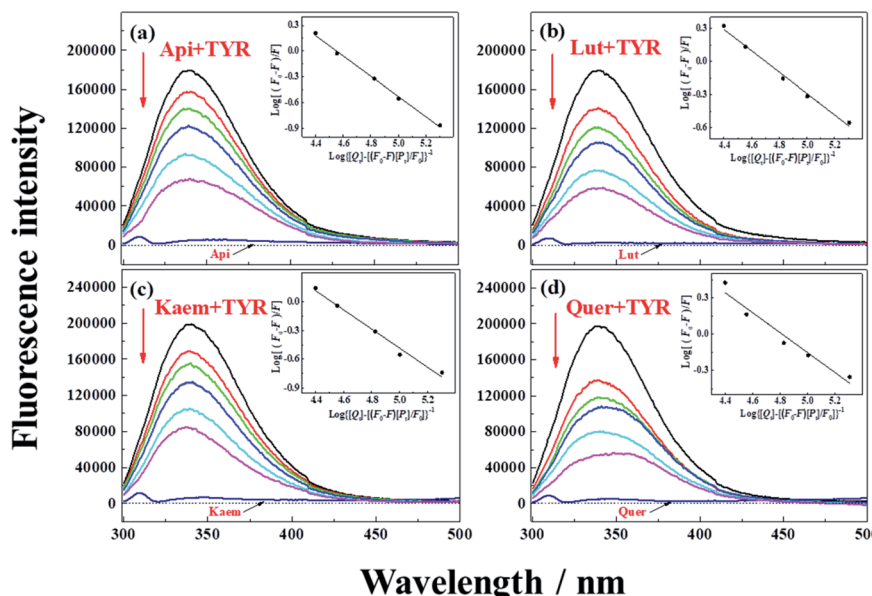


**Fig. 2** Fluorescence emission spectra of  $28 \mu\text{g mL}^{-1}$  tyrosinase in the presence of varying concentrations,  $0, 5, 10, 15, 28, 40 \mu\text{M}$  (a) Api, (b) Lut, (c) Kaem and (d) Quer at  $25^\circ\text{C}$ , respectively.  $\lambda_{\text{ex}} = 280 \text{ nm}$ . Insets: plots of  $\log[(F_0 - F)/F]$  at  $\lambda_{\text{em}} = 340 \text{ nm}$  according to the double-logarithm eqn (3).  $F_0$  and  $F$  represent fluorescence intensities of solutions in the absence and presence of flavonoids.



where  $F$  and  $F_m$  represent the calibrated and measured fluorescence intensity;  $A_1$  and  $A_2$  stand for the absorbance at the excitation wavelength ( $\lambda_{ex} = 280$  nm) and emission wavelengths of flavonoids, respectively.

Tyrosinase in aqueous solution was found having a strong fluorescence emission peak at 340 nm, while flavonoids showed little fluorescence emission under the same conditions. The fluorescence intensities of tyrosinase significantly decrease with increasing concentrations of flavonoids, indicating that flavonoids quench the fluorescence of tyrosinase. No obvious changes observed in the calibrated fluorescence emission spectra of tyrosinase, indicating the interaction of flavonoids with tyrosinase almost not altering the proximal environment of the chromophore tryptophan residues.

The quenching constants,  $K_q$ , of flavonoids with tyrosinase were determined by linear fitting the fluorescence intensity ratio ( $F_0/F$ ) using the Stern–Volmer eqn (2) below:<sup>17,36</sup>

$$\frac{F_0}{F} = 1 + K_q \tau_0 [Q] \quad (2)$$

$F_0$  and  $F$  are the fluorescence intensities of tyrosinase in the absence and presence of flavonoids, respectively.  $K_q$ ,  $\tau_0$  and  $[Q]$  are the bimolecular quenching constant, the average lifetime of the fluorophore without the quencher  $\tau_0 = 10$  ns (ref. 36) and the concentration of the quencher, respectively.

The obtained quenching constants,  $K_q$ , of the four flavonoids with tyrosinase,  $4.19 \times 10^{12}$  L mol<sup>-1</sup> s<sup>-1</sup> for Api,  $5.19 \times 10^{12}$  L mol<sup>-1</sup> s<sup>-1</sup> for Lut,  $3.47 \times 10^{12}$  L mol<sup>-1</sup> s<sup>-1</sup> for Kaem and  $6.13 \times$

$10^{12}$  L mol<sup>-1</sup> s<sup>-1</sup> for Quer, are higher than the maximum diffusion collision quenching constant ( $2.0 \times 10^{12}$  L mol<sup>-1</sup> s<sup>-1</sup>),<sup>17</sup> indicating that the fluorescence quenching of tyrosinase by the four flavonoids in this study is a static process. The binding constant ( $K_a$ ) and the number of binding sites ( $n$ ) for static quenching of flavonoids with tyrosinase were calculated by linear regression of the plot of  $\log \frac{F_0 - F}{F}$  against  $\log \frac{1}{[Q_t] - \frac{(F_0 - F)[P_t]}{F_0}}$  following the double-logarithm eqn (3) as shown in Fig. 2a–d insets<sup>26,37</sup>

$$\log \frac{F_0 - F}{F} = n \log K_a - n \log \frac{1}{[Q_t] - \frac{(F_0 - F)[P_t]}{F_0}} \quad (3)$$

where  $F_0$  and  $F$  are the same as in eqn (2), and  $[Q_t]$ ,  $[P_t]$  are the total concentrations of flavonoids and tyrosinase, respectively.  $K_a$  and  $n$  were approximately determined to be  $K_a = 3.57 \times 10^4$ ,  $5.01 \times 10^4$ ,  $3.26 \times 10^4$  and  $6.53 \times 10^4$  L mol<sup>-1</sup> and  $n = 1.18$ , 0.97, 0.99 and 0.83 for Api, Lut, Kaem and Quer, respectively. These results support one tyrosinase binds with one flavonoid molecule in agreement with ref. 26.

### Enzymic oxidation of flavonoids by tyrosinase

Reactions between Api, Lut, Kaem and Quer with tyrosinase were followed spectrophotometrically for air-saturated solutions as shown in Fig. 3a–h in comparison with the

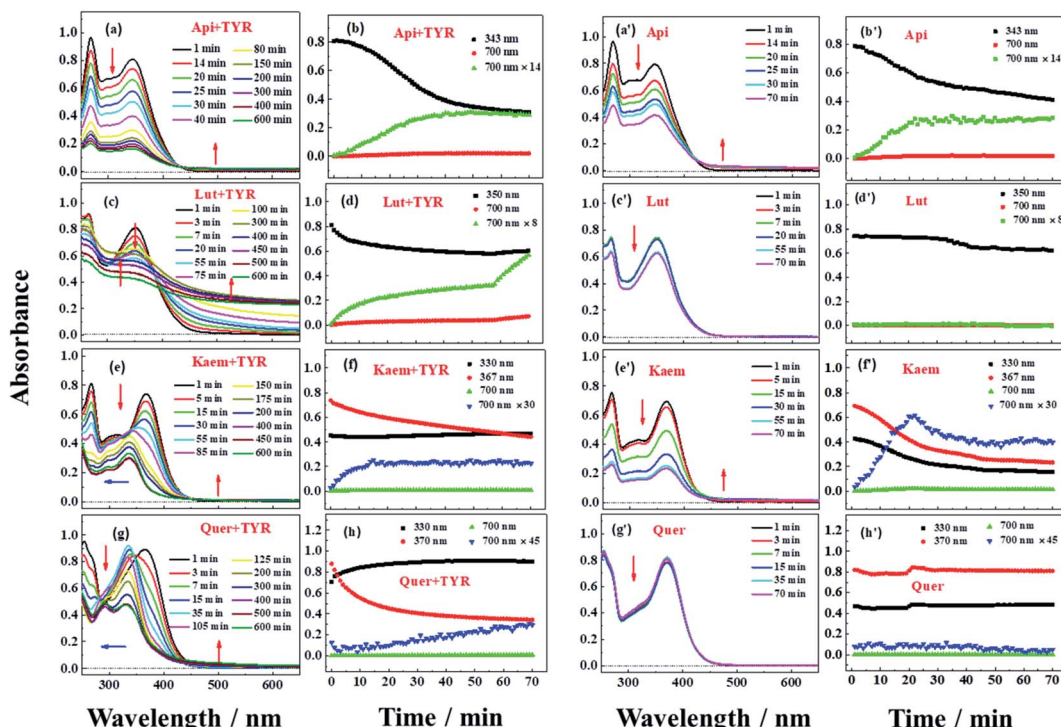


Fig. 3 Absorption spectra (a, c, e and g) and absorption changes (b, d, f and h) for  $28 \mu\text{g mL}^{-1}$  tyrosinase reacting in air-saturated aqueous solution with  $100 \mu\text{M}$  Api, Lut, Kaem and Quer, respectively, at  $25^\circ\text{C}$ . The absorption spectra (a', c', e' and g') and absorption changes (b', d', f' and h') for the autoxidation of  $100 \mu\text{M}$  Api, Lut, Kaem and Quer alone, were shown for comparison. The absorption changes at 700 nm are enlarged for clarity. The optical length of the quartz cells is 0.5 cm.



autoxidation of flavonoids alone by oxygen in air as shown in Figure 3a'–h'. The detailed mechanism including the enzymatic oxidation and autoxidation of Api, Lut, Kaem and Quer is summarized in Scheme 2.

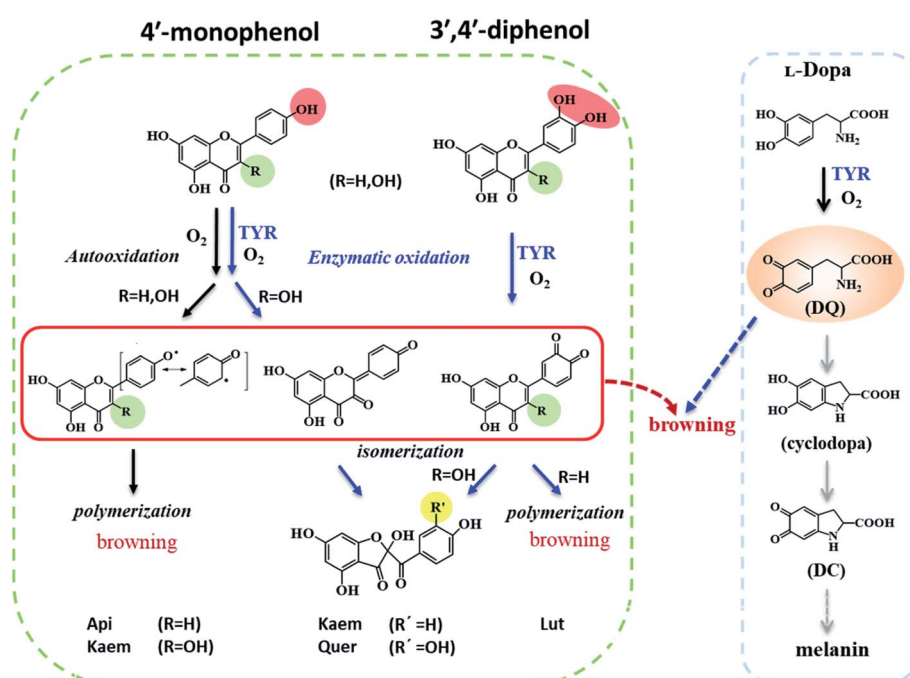
The reactivity of the tyrosinase toward each compound differed significantly. Continuous changes in absorptions spectra (Fig. 3a, c, e and g) show that oxidation occurs after addition of flavonoids to tyrosinase, which are different from reaction of flavonoids with Cu(II) or other metal ions forming relatively stable flavonoid complexes as found in our previous studies.<sup>38–41</sup> In contrast, the autoxidation of flavonoids alone are less complicated.

During both enzymatic oxidation and autoxidation of Api (Fig. 3a and a'), similar small changes in the character of the absorption spectra but with larger reduction in the absorption intensity at 250–450 nm and with a slight increase in absorbance intensity at longer wavelength. The brown product absorbing at longer wavelength is assigned as a flavonoid dimer or polymer formed from an oxidized flavonoid, phenoxyl or quinone radical, reacting with other parent flavonoid molecules or dimerization of flavonoid quinones themselves.<sup>42–46</sup> The dimerization or polymerization of Api are thus suggested to occur *via* an oxidation intermediate of the most reducing 4'-phenol, 4'-monoquinone. The kinetics at 343 nm and the enlarged kinetics at 700 nm in Fig. 3b and b' both show the correlation of the decay of the parent Api and the formation of the brown polymerized flavonoids in similar amount. The rate obtained from the kinetics at 700 nm in enzymatic oxidation is slightly slower than for the autoxidation (Fig. 3b and b'), indicating that the interaction of Api with tyrosinase almost does not change the reaction pathway of autoxidation, but only

slightly slows down the reaction rate of autoxidation by a weak interaction.

In case of Lut containing a catechol group of ring B but lacking a 3-hydroxyl group of ring C, the absorption intensity at wavelengths lower than 400 nm decreased faster than for Api during enzymatic oxidation although the change in the characteristic of absorption spectra were similar as seen in Fig. 3c. The kinetics followed by spectral changes at 350 nm and the enlarged kinetics at 700 nm at less than 60 min also shows good correlation, which is similar to Api for the decay of the parent Lut and for the formation of the polymerized products (Fig. 3d). The absorption spectra at 700 nm for Lut increased more significantly than for Api, and after 60 min the otherwise homogeneous solution begins to be flocculent with brown precipitate. In contrast, the autoxidation of Lut is far less distinctive than autoxidation of Api as seen spectral changes at 250–450 nm, and almost no brown product seems to be formed following absorption at longer wavelength as seen Fig. 3c' and d'. Lut as well as eriodictyol and catechin both containing catechol group have been reported to be enzymatically oxidized into *o*-dquinone, which is reactive and tends to react with the parent Lut forming polymerized products.<sup>43–46</sup> This may be explained by the stronger absorbance noted for Lut at the longer wavelength than for other flavonoids under consideration. The reaction of monophenol in ring B of Api oxidized into diphenol forming Lut, is excluded due to differences in spectral changes obtained for Api with Lut at longer times.

The spectra peaked at ~370 nm for Kaem and Quer containing 3-hydroxyl group of ring C during enzymatic oxidation and gradually blueshifted, similar to what has been characterized to form of the protocatechuate products 2-(3,4-



**Scheme 2** Proposed mechanism of autoxidation and enzymatic oxidation of flavonoids and promotion effect of flavonoids on browning induced by enzymatic oxidation of L-dopa.



dihydroxybenzoyl)-2,4,6-trihydroxy-3(2*H*)benzofuranone with an absorption maximum at 330 nm (Fig. 3e and g) *via* intermediates, monoquinone for Kaem and diquinone for Quer, by electrochemical and enzymatic oxidation.<sup>27,47</sup> Whereas, the autoxidation of Kaem has similar spectral changes as Api both containing 4' mono-phenol in ring B and showing the obvious decrease in absorption intensity of parent molecules at shorter wavelength and observable increase of the polymerized products at longer wavelength (Fig. 3a' and e'). No isomerized protocatechuate products are observed in autoxidation and there is far more oxidized brown product formed a little later in autoxidation than in enzymatic oxidation, as seen from the time trace of absorption at 700 nm shown in Fig. 3f and f'. This difference in kinetics implicates that enzymatic oxidation is more favorable. Kaem has a 3-hydroxyl group as one more reactive site when compared to autoxidation resulting in isomerization into protocatechuate products, which inhibits the brown product formed with absorption at longer wavelength. Notably, the autoxidation of Quer shows similar and indistinctive spectral changes as Lut both containing 3',4'-catechol group in ring B (Fig. 3c', d', g' and h'). Due to the weak reactivity in reaction with oxygen and resistance against autoxidation, Quer still containing a catechol diphenol group is more reactive towards enzymatically forming protocatechuate products than Kaem containing the 4'-monophenol group.

As seen in Scheme 2, Api and Kaem with 4'-monophenol in ring B are autoxidized faster and more than Lut and Quer with the 3',4'-diphenol moiety. Enzymatic oxidation of 4'-monophenol in Api and Kaem yields 4'-phenoxy or quinone radicals while the 3',4'-diphenol of Lut and Quer forms 3',4'-diquinone. Enzymatic oxidation of 4'-monophenol in Kaem and 3',4'-diphenol in Quer to form monoquinone and diquinone, respectively, followed by isomerization into protocatechuate products, is accordingly more favorable than autoxidation of both Kaem and Quer.

### Effects of flavonoids on enzymic oxidation of L-dopa induced by tyrosinase

UV-vis spectra and their changes after addition of 2000  $\mu$ M L-dopa to the solutions of 28  $\mu$ g mL<sup>-1</sup> tyrosinase without and with 100  $\mu$ M Api, Lut, Kaem and Quer pre-incubated for 5 min were recorded and the changing spectra are shown in Fig. 4a–e and 5a–c, respectively.

An absorption peak with maximum at 480 nm appeared upon addition of L-dopa to tyrosinase (Fig. 4a). This species has been well established as an intermediate of the enzymatic reaction, DC, during melanin formation from oxidation of dopaquinone (DQ) followed by oxidation of cyclodopa, reaching a concentration maximum in 5 minutes and subsequently decaying and transforming into melanin with absorption

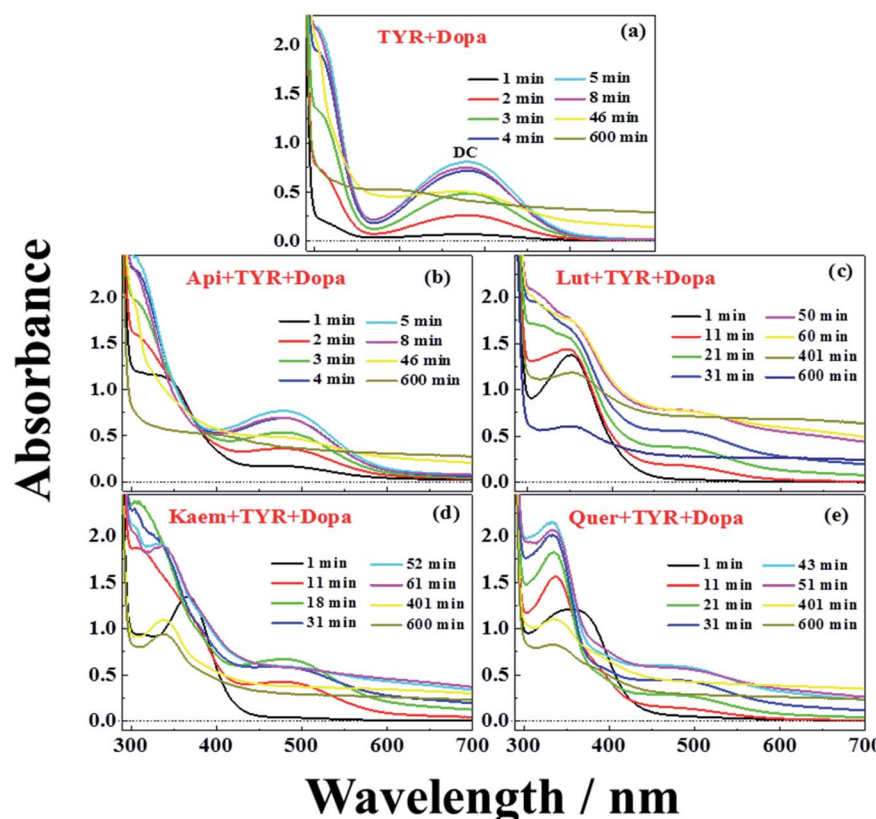


Fig. 4 Absorption spectra during oxidation of 2000  $\mu$ M L-dopa by 28  $\mu$ g mL<sup>-1</sup> tyrosinase (a) in the absence of flavonoids, and in the presence of 100  $\mu$ M (b) Api, (c) Lut, (d) Kaem, (e) Quer pre-incubated at 25 °C in air-saturated solution. The mixture of tyrosinase and flavonoids were pre-incubated for 5 min before adding L-dopa. The optical length of the quartz cells is 1 cm.



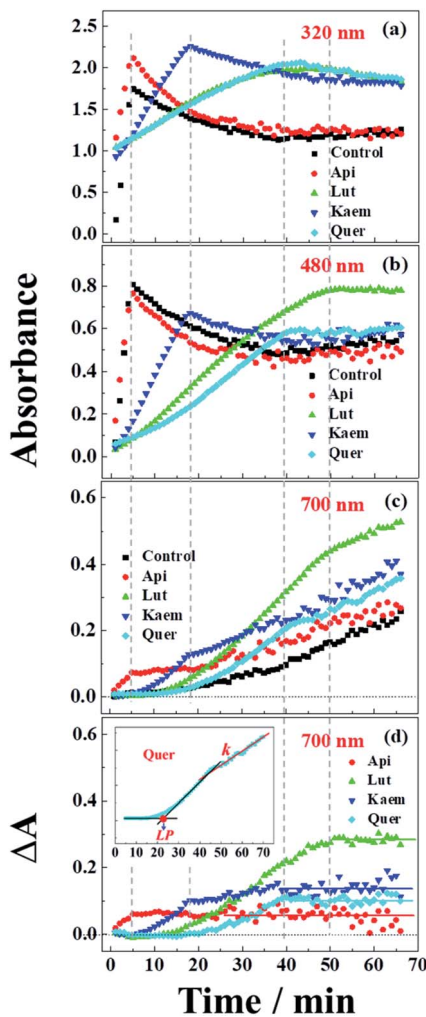


Fig. 5 Absorbance changes at (a) 320 nm, (b) 480 nm and (c) 700 nm as extracted from spectra of Fig. 4b–d and (d) absorption differences between the samples with flavonoids and without flavonoids at 700 nm. Control in a–c is the kinetics from Fig. 4a. Insets: Quer as an example to indicate the methods used to determine the lag phase, LP in min, and the rate constant,  $k$  in  $\text{min}^{-1}$ , of the linear increase in the region after the inflection point.

ranging from 300 nm to 700 nm *via* multi-step polymerization (Scheme 2). In this process, only the characteristic absorption of DC (300–500 nm) and of melanin (300–800 nm) were observed

**Table 1** Binding constant ( $K_a$ ,  $\text{L mol}^{-1}$ ) and binding number ( $n$ ) of flavonoids with tyrosinase obtained from the fluorescence of tyrosinase quenched by flavonoids. The inflection time at 700 nm,  $t_t$  for the ternary system (tyrosinase, flavonoids and L-dopa),  $t_e$  for enzymatic oxidation (tyrosinase and flavonoids), and  $t_a$  for autooxidation of flavonoids alone. Absorbances at 700 nm and at 70 min,  $A_t$  for the ternary system,  $A_e$  for enzymatic oxidation and  $A_a$  for autooxidation. Lag phase (LP, min) prior to the increasing absorbance at 700 nm and rate constants ( $k$ ,  $\text{min}^{-1}$ ) by linear fitting of the increasing absorbance for samples without flavonoids and with flavonoids after the inflection point at 700 nm in Fig. 5c. The absorbance difference,  $\Delta A_t$  obtained from the constant absorbance seen in Fig. 5d by subtracting the absorbance of the sample without flavonoids from the absorbance of the samples with flavonoids<sup>a</sup>

Flavonoid	$K_a$ ( $\times 10^4$ , $\text{L mol}^{-1}$ )	$n$	$t_t$ (min)	$t_e$ (min)	$t_a$ (min)	$A_t^*$	$A_e^{\#}$	$A_a^{\#}$	LP <sub>t</sub> (min)	$k_t$ ( $\times 10^{-3}$ , $\text{min}^{-1}$ )	$\Delta A_t$
Api	3.57	1.18	9	32	22	0.076	0.042	0.042	5	4.79 ± 0.28	0.063
Lut	5.01	0.97	53	12	—	0.434	0.142	0.003	20	5.50 ± 0.08	0.288
Kaem	3.26	0.99	21	9	22	0.129	0.014	0.024	11	6.18 ± 0.23	0.148
Quer	6.53	0.83	47	—	—	0.237	0.014	0.014	22	6.19 ± 0.09	0.111
Blank									24		5.66 ± 0.13

<sup>a</sup> \* and # represent using 1 cm and 0.5 cm, respectively.  $A_e$  and  $A_a$  are enlarged two times for comparison with the absorbance of the ternary system,  $A_t$ . “—” means undetectable due to lower absorbance close to baseline or lack of inflection time.

due to the formation of intermediates, DQ and cyclodopa, occurring at a shorter timescale with a first order rate constant of  $5.2 \times 10^{-3} \text{ min}^{-1}$ .<sup>6</sup> The detailed transformation mechanism have been investigated by real time kinetic studies using Raman and UV-vis spectra recently.<sup>6</sup> Similar dynamics are also obtained in the present study and shown as “control” in Fig. 5a–c.

Upon addition of L-dopa to tyrosinase pre-incubated with flavonoids, it is evident that for the four flavonoids, the absorption spectra from 350 nm to 700 nm decreases in intensity and broadens to a varying degree as seen Fig. 4b–e. The same inflection points for the four flavonoids at the same delay time were observed for the dynamics at 320 nm, 480 nm and 700 nm show obvious correlation between the intermediates and products formed in enzymatic reaction as shown Fig. 5a–c, also supporting formation of an oxidized intermediate and interference of product absorption in the same spectral region. Kinetics as followed at 320 nm seems too complicated to be analyzed due to the spectral overlap of flavonoids, L-dopa, DC and melanin. The formation and decay kinetics of DC at 480 nm is in contrast widely accepted as a standard for quantification of the inhibitory efficiencies of tyrosinase inhibitors. The kinetic inhibition effects as followed at 480 nm for the four flavonoids are Quer > Lut > Kaem > Api (cf. Fig. 5b), which is consistent with the binding constants for Api and Kaem lower than for Lut, and far lower than for Quer (Table 1).

It should be noted that the dynamics in ternary system as followed spectroscopically at 480 nm for L-dopa enzymatically oxidized by tyrosinase pre-incubated with Api only shows slightly smaller changes than as seen for the sample enzymatically oxidized by tyrosinase alone (Fig. 5b). However, an obvious increase in spectral changes in ternary system at 700 nm for Api gives an inflection time,  $t_t = 9$  min, notably far earlier than the slow formation of melanin for samples without Api added and also earlier than inflection times as seen in the spectra,  $t_e = 32$  min and  $t_a = 22$  min, for the formation of the products from enzymatic oxidation and autooxidation of Api, respectively (Fig. 3b and b', 5c and Table 1). The absorbance at 700 nm in ternary system is also higher than enzymatic oxidation and autooxidation of Api by comparing the absorbance intensity at 700 nm and at 70 min,  $A_t$  for ternary system,  $A_e$  for



enzymatic oxidation and  $A_a$  for autoxidation, as seen in Table 1. This implicates there is more active reactant involving the reaction with phenoxyl or quinone radical of Api to yield brown product. The new brown product at 700 nm is excluded as formation from the enzymatic oxidation of L-dopa alone (control in Fig. 5c) or from enzymatic oxidation and autoxidation of Api. In addition, no absorbance is appearing at 700 nm for the products of parent flavonoids reaction with the enzymatically oxidized species *o*-quinones of L-dopa, dopaquinone (DQ), as reported by Gąsowska-Bajger *et al.*<sup>27</sup> A product from the reaction of oxidized Api, monoquinone, with DQ, is suggested to be responsible for the brown product at 700 nm as evidenced by a reaction of chlorogenic acid quinone with catechin quinone leading to enzymatic browning of apple,<sup>44</sup> and by the HPLC-MS results with Lut as an example, which will be further explained in the following.

Similarly the more remarkable absorbance at longer wavelength also suggests that a reaction of oxidized flavonoids, monoquinone for Kaem and diquinone for Lut and Quer, occurs with DQ. This absorption was also observed for samples of L-dopa and tyrosinase pre-incubated with the other three flavonoids including Kaem, Lut and Quer by comparing the absorbance at 700 nm of the ternary system with enzymatic oxidation and autoxidation,  $A_t \gg A_e \sim A_a$  (Table 1). The kinetic inflection points of time in ternary system for Kaem, Lut and Quer, however, are found longer than in enzymatic oxidation and autoxidation, which may arise from stronger binding of flavonoids with tyrosinase (Table 1). A lag phase LP (in min) was determined from the intersecting point of the slope line at the middle point with the baseline, as shown in Fig. 5d inset with Quer as an example. LP values of 5, 20, 11, 22 min for Api, Lut, Kaem, Quer, respectively, as listed in Table 1 shows distinct effects. Compared with Api, the prolonged LP corresponding to the slower formation of brown product may arise from the increasingly stronger binding of 3,4 conjugation or catechol groups for Kaem, Lut and Quer with Cu(II) ion of tyrosinase compared to binding at the 4,5 group in Api. Higher absorbance of the brown product may therefore be ascribed to the higher reactivity with DQ of the products formed from enzymatic oxidation probably accompanying with autoxidation, monoquinone for Kaem and diquinones for Lut and Quer, respectively, compared with monoquinone for Api.

It is also clearly seen from kinetics monitored at 700 nm in Fig. 5c that the linearly increasing absorption at the timescale after the inflection point for all samples with flavonoids are almost in parallel with the absorption changes for the sample without flavonoids. The rate constants,  $k$ , obtained by linear fitting the spectral changes after the inflection time (inset in Fig. 5d) shown in Table 1 implicate all samples has the similar reaction rates for melanin formation. Accordingly, the involvement of flavonoids in the system of L-dopa and tyrosinase almost do not affect the formation of melanin. The results of the kinetics as followed at 700 nm for samples with flavonoids subtracting the kinetics for the sample without flavonoids evidently gives the rate of formation of the new brown product, formed from flavonoid quinone reaction with dopaquinone reaching constant absorbance within 70 min. Lut is found to

have the most distinct effect on promotion of browning followed by Kaem, Quer and Api, on the basis of constant absorbance of the difference kinetics at 55–70 min in ternary system,  $\Delta A_t$ , as seen in Fig. 5d and Table 1. Lut containing 3',4'-diphenol group is enzymatically oxidized into diquinone, showing the highest reactivity to react with dopaquinone leading to browning. Kaem ranks second among four flavonoids due to the integrated contributions from the reaction of monoquinone of Kaem with dopaquinone and from its autoxidation and competition with isomerization into protocatechuate products from monoquinone of Kaem. Lower absorbance for Quer may arise from its lower reactivity in browning by autoxidation although Quer shows similar reactivities of diquinone with dopaquinone and similar isomerization from diquinone. Api shows the least promotion effect in browning, which may be due to the weak interaction of tyrosinase with parent Api.

#### HPLC-mass analysis of the products of enzymatic oxidation

HPLC-MS was performed with Lut as an example due to more obvious formation of browning products at 700 nm for Lut compared to other flavonoids (Fig. 5d).

Enzymatic oxidation products at 70 min of elution for L-dopa and for Lut individually, and for L-dopa and Lut together by tyrosinase under the same conditions as the experiment of Fig. 3c and 4a and c were analyzed by HPLC-MS. As seen in HPLC spectra of Fig. 6a, when compared with the binary

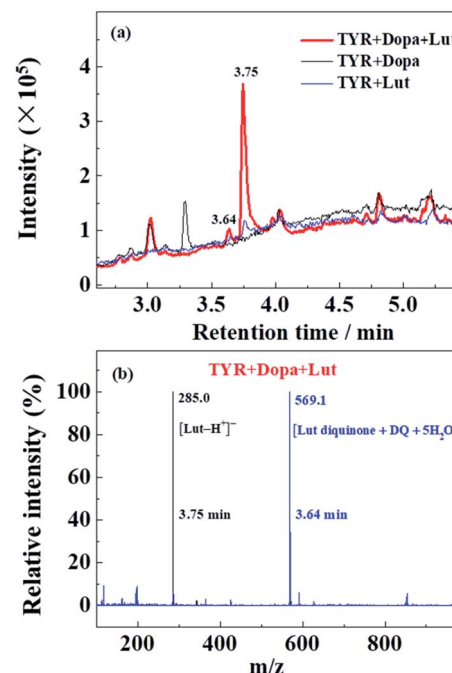


Fig. 6 (a) HPLC-MS spectra of enzymatic oxidation of 2000  $\mu$ M L-dopa and of 100  $\mu$ M Lut individually by 28  $\mu$ g mL<sup>-1</sup> tyrosinase, and of 2000  $\mu$ M L-dopa addition to 28  $\mu$ g mL<sup>-1</sup> tyrosinase pre-incubated with 100  $\mu$ M Lut for 5 min at 25 °C in air-saturated solution. The reaction time of all samples for HPLC-MS determination is 70 min. (b) MS spectra of the ternary system of tyrosinase, Lut and L-dopa in (a) at 3.75 min and 3.64 min.



systems of L-dopa or Lut oxidized by tyrosinase, the ternary system of L-dopa, Lut and tyrosinase has a new component appearing at 3.64 min of elution and has a distinctly stronger component at 3.75 min. MS spectra in Fig. 6b shows the component at 3.75 min is the parent Lut, which may arise from the enzymatic oxidation of Lut inhibited by addition of L-dopa. More parent Lut is left in the ternary system compared to most of Lut oxidized by tyrosinase in the binary system. The MS spectra at 3.64 min in Fig. 6b gives a 569.1 negative ion peak. This component is explained as a complex formed from combination of an enzymatically oxidized Lut, *o*-dquinone and an oxidized L-dopa, DQ together with five water molecules, [Lut diquinone + DQ + 5H<sub>2</sub>O]<sup>-</sup>, in agreement with the above assignments in the kinetic analysis. This complex is not further characterized in more detail in present study.

The detailed reaction mechanism of four flavonoids involving the catalytic oxidation of L-dopa by tyrosinase is also summarized in Scheme 2.

### Effect of flavonoids on browning of white mushroom slices

The effects of flavonoids on the browning of white mushrooms were followed with intervals of one hour recording the changes in color and in spectra for up to 8 hours by the use of a camera and the diffuse reflectance spectroscopy, respectively. It is seen from the photographs at 0, 2 and 8 hours in Fig. 7 that the color of all mushroom slices turns brown as time increases. All mushroom slices at 8 hours show atrophy to varying extent due to the vaporization of moisture. The mushrooms soaked in flavonoid solutions turned brown faster than mushrooms soaked in PBS solution alone, which was especially evident for Kaem and Quer. The sample soaked in Lut is marginally less brown than samples soaked in Kaem and Quer, and the sample soaked in Api is far less brown.

The absorption spectra at 2 and 8 hours and spectral changes at 480 nm and 700 nm quantitatively measured by diffuse reflection in Fig. 8a-d show that the absorbance of the mushroom slices soaked in the flavonoid solutions were higher than for the slices only soaked in PBS buffer. The absorbance intensity for the samples soaked in solutions of the four investigated flavonoids have comparable intensity at 2 hours, but marginally higher for Lut, Kaem and Quer than Api after 8 hours. This increasing absorbance intensity in the presence of

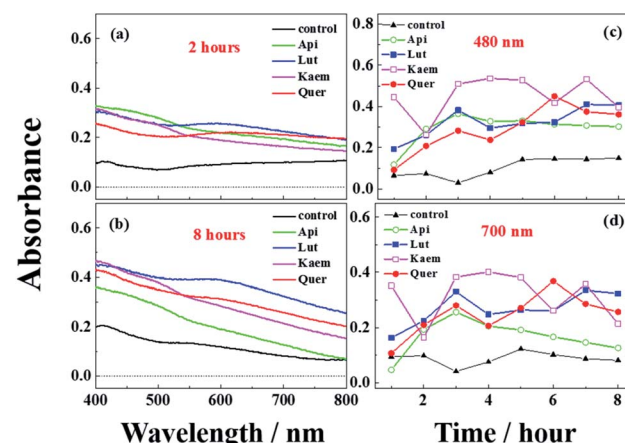


Fig. 8 Diffuse reflectance spectra (a and b) and absorption changes at 480 and 700 nm (c and d) recorded for mushrooms soaked in solutions without and with 100  $\mu$ M Api, Lut, Kaem, and Quer for 10 min at 25 °C in air-saturated water. All solutions are 100  $\mu$ M PBS buffer containing 5% DMSO to increase the solubility of flavonoids. Control in a-d is the sample immersed in PBS buffer only.

flavonoids observed by diffuse reflection is consistent with the changes in color shown in Fig. 7.

### Discussion

Flavonoids have been confirmed to be both oxidation substrates and inhibitors of tyrosinase. The enzyme inhibitory kinetics has shown that almost all flavonoids have more or less significant inhibitory effects on tyrosinase by monitoring the formation and decay at  $\sim$ 480 nm of the DC reaction intermediate. However, in the present study, four structure-related flavonoids, Api, Lut, Kaem and Quer were confirmed to promote not inhibit the enzymatic browning both in model and food systems by comparing the spectral changes in ternary system including L-dopa, tyrosinase and flavonoids with enzymatic oxidation and autoxidation of flavonoids and with mushroom slices.

The reaction conditions including the concentration range selected for the present investigation are comparable to the conditions used by others.<sup>17,18,48,49</sup> Similar pseudo inhibition effects were also observed if the kinetics was only monitored at a single wavelength of 480 nm. This wavelength has been confirmed to contain contribution to absorption or a variety of components including DC, DQ and melanin, making the wavelength inaccurate for analysis of melanin formation. The kinetics followed at 700 nm help to exclude the interference from absorbance of DC. The combination of analysis of kinetics at 480 nm and 700 nm further helped to distinguish the formation of melanin from other transformations. This conclusion is also supported by the experiment involving mushroom browning as a real food system.

During the autoxidation of flavonoids alone, Api and Kaem with 4'-mono-phenol in ring B is more susceptible to be oxidized by oxygen in air than Lut and Quer with 3',4' di-phenol in ring B. 3',4' di-phenol facilitating to stabilize the structures of Lut and Quer in the process of autoxidation, although they

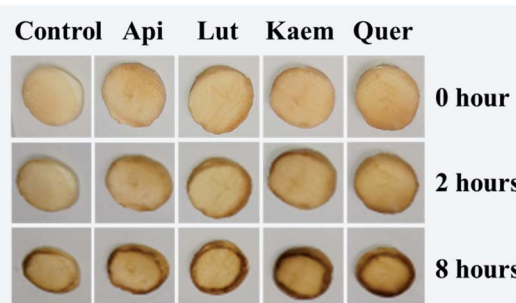


Fig. 7 Changes in color for mushroom cap/pileus slices after being soaked in solutions without and with 100  $\mu$ M Api, Lut, Kaem or Quer in PBS buffer with 5% DMSO for 10 min in air at 25 °C.



generally show higher radical scavenging activities than phenols in Api and Kaem.<sup>50</sup>

In the enzymatic oxidation of flavonoids as substrates, tyrosinase shows low reactivity in oxidation of Api and the character of the spectral changes are almost similar to the changes in the autoxidation. High reactivity of tyrosinase to oxidize Kaem into monoquinone followed by isomerization competing with autoxidation lead to less effect on browning than autoxidation. Lut containing the catechol group more easily enzymatically forms diquinone leading to more distinct browning by polymerization than Api and Kaem without the catechol. Quer, despite containing a catechol group also easily forms diquinone like Lut, shows less browning tendency due to the competition of isomerization with polymerization.

In the binary system of L-dopa as substrates of tyrosinase, the decay of the reaction intermediate DC results in the formation of the brown product, melanin, occurring at 24 min as shown in Fig. 5c and Table 1.

In the ternary system of L-dopa and tyrosinase pre-incubated with flavonoids, flavonoids as both substrates and inhibitors of tyrosinase react competitively with L-dopa, otherwise reacting with tyrosinase. Comparing the results for the enzymatic oxidation and autoxidation of flavonoids and enzymatic oxidation of L-dopa, new brown products for the ternary system appear at 5–22 min as detected for the first time in present study (Fig. 5d and Table 1), and earlier than the formation of melanin, which further promote the browning of the samples. The new brown products do not form from the enzymatic oxidation of individual flavonoids or L-dopa alone. The reaction of flavonoids with dopaquinone (DQ) as reported in ref. 27 was also excluded by the results of the present study based on the spectral comparison, showing no absorption at higher wavelengths than 600 nm for the product of flavonoid reacting with DQ. An oxidized product of flavonoids as substrates, quinones of flavonoid, is now suggested to react with the oxidized product of L-dopa as substrates, DQ, both produced from enzymatic oxidation of tyrosinase, forming the brown complexes as shown in Scheme 2, and thus promote not inhibit browning.

DQ reacts with quinones of flavonoids promoting browning, however, seems to slow down the formation of DC at 480 nm and therefore shows inhibition effects. This inhibition effect depends on secondary reactions and cannot be assigned to the inhibition reactivities of flavonoids as otherwise reported.<sup>27</sup> DQ has been found to trigger neuronal damage in the brain due to dopaminergic neurons deficiency in turn leading to Parkinson diseases.<sup>18,51</sup> Reaction of enzymatically oxidized flavonoid with DQ may give a new perspective for further understanding flavonoids as bioactive molecules with health protecting effects.

The spectral changes at longer time after the respective inflection points (Fig. 5c and Table 1) are almost parallel with the rate constants for Api, Lut, Kaem and Quer obtained by linear regression, indicating that addition of flavonoids hardly affects the rate of melanin formation from enzymatic oxidation of L-dopa when in excess. The small differences in observed kinetics between samples with and without flavonoids suggest a common mechanism including fast formation and a similar constant concentration of the brown complex for all flavonoids

(Fig. 5d). This result indirectly supports the validity of the assumption that melanin formation is not affected by flavonoids in presence of excessive L-dopa. Flavonoids does not seem to inhibit formation of melanin deactivating tyrosinase, but are oxidized into quinones to react with DQ forming a complex to promote browning instead.

## Conclusions

The four flavonoids, Api, Kaem, Lut and Quer, have significantly different effect on autoxidation and enzymatic oxidation both as substrates and as inhibitors of tyrosinase, and also in their effect on melanin formation leading to browning. Flavonoids with 4'-monophenol groups, Api and Kaem, are more readily autoxidized and polymerized into browning products than Lut and Quer. On the contrary, enzymatic oxidation of flavonoids alone almost has no effect on Api, for which flavonoid autoxidation still is dominant, while Lut containing the catechol group is far more easily oxidized into diquinone compared to autoxidation leading to distinct browning through polymerization. Flavonols, both Kaem and Quer with 3-hydroxyl are enzymatically oxidized into mono or diquinone, which further isomerizes into products absorbing at lower wavelength resulting in formation of product with paler brown color and different from autoxidation product of Kaem or enzymatic oxidation product of Lut. Notably, Quer containing a catechol like Lut, behaves more like Kaem than like Lut.

When L-dopa added as a substrate competes with flavonoids as substrate for tyrosinase, the four flavonoids are all expected to promote browning through formation of complexes by combination of the quinones of the oxidized flavonoid with DQ. Browning promotion effects of the four flavonoids as studied in model systems are also observed for mushrooms as a relevant food system. This study may accordingly provide new perspectives for flavonoids as important food components, and as enzymatic inhibitors, additives and as antioxidants in food.

## Materials and methods

### Materials and reagents

Kaempferol (Kaem, >98%), apigenin (Api, >98%), luteolin (Lut, >98%) and quercetin (Quer, >98%) were from Huike Plant Exploitation Inc., (Shanxi, China). Mushroom tyrosinase (TYR, 7164 units/mg) was purchased from Sigma Chemical Co. (St. Louis, USA). L-Dopa was purchased from Sangon Biotech (Shanghai) Co. Ltd. Dimethyl sulfoxide (DMSO) was purchased from Aladdin Chemicals Co. (Shanghai, China). Phosphate buffer solution (PBS, ≥99.5%) was from Coolaber Co. (Beijing, China). Fresh white mushroom were bought from supermarket. The cap/pileus of white mushroom were uniform cut into slices with thickness of 2 mm and diameter of 12 mm by the combined use of an electric slicer and a perforator.

### Fluorescence of tyrosinase quenched by flavonoids

Fluorescence spectra were measured using a FLS980 fluorescence spectrophotometer (Edinburgh Instruments, UK). The



concentration of tyrosinase is  $28 \mu\text{g mL}^{-1}$  and the concentration of flavonoids ranges from 0 to  $40 \mu\text{M}$ . The excitation wavelength  $\lambda_{\text{ex}}$  is 280 nm. The fluorescence spectra of all samples were corrected by subtracting the spectra of sodium phosphate buffer alone.

### Enzymatic oxidation of flavonoids and L-dopa pre-incubated with flavonoids by tyrosinase

Tyrosinase and flavonoids (Api, Lut, Kaem, Quer) were mixed in 50 mM phosphate buffer at pH 6.8. The final concentrations are 100  $\mu\text{M}$  for flavonoids, and  $28 \mu\text{g mL}^{-1}$  for tyrosinase. 3% (v/v) DMSO was used to increase the solubility of flavonoids in buffer. All absorption spectra were obtained every minute.

UV-vis absorption spectra of enzymatic oxidation of flavonoids by tyrosinase in binary system and enzymatic oxidation of L-dopa by tyrosinase pre-incubated with flavonoids in ternary system were recorded on a Cary60 spectrophotometer (Varian, Inc., Palo Alto, CA, USA) using 0.5 and 1.0 cm quartz cells at 25 °C, respectively. The autoxidation of flavonoids alone in the same concentrations are also performed for comparison using 0.5 cm quartz.

Tyrosinase and flavonoids (Api, Lut, Kaem, Quer) were mixed and incubated at 25 °C for 5 minutes. L-dopa was added to pretreated solution of tyrosinase and flavonoids, and the absorption spectra were recorded every minute using 50 mM aqueous phosphate buffer as solvent (pH 6.8). The final concentrations are 100  $\mu\text{M}$  for flavonoids,  $28 \mu\text{g mL}^{-1}$  for tyrosinase and 2000  $\mu\text{M}$  for L-dopa. 3% (v/v) DMSO was used to increase the solubility of flavonoids.

Enzymatic oxidation of 2000  $\mu\text{M}$  L-dopa alone by  $28 \mu\text{g mL}^{-1}$  tyrosinase was also recorded in parallel for comparison.

### HPLC-mass analysis of the products of enzymatic oxidation

The samples were prepared under the same experimental conditions as above mentioned enzymatic oxidation of Lut and L-dopa individually, and oxidation of L-dopa by tyrosinase pre-incubated with Lut, respectively. 100  $\mu\text{L}$  reaction mixtures for the three samples at 70 min were analyzed on HPLC-MS (Ultimate 3000 UHPLC-Q Exactive, Thermo Scientific, US) equipped with a Zorbax 300SB-C8 column (250 mm  $\times$   $\phi$  4.6 mm; size of immobile particles,  $\phi$  5  $\mu\text{m}$ ). The mobile phases were 0.1% formic acid in water as the A-phase, and acetonitrile as the B-phase. The determination conditions for HPLC were as follows: 5% A + 95% B for 0–1 min; 55% A + 45% B for 1–3 min; 100% A for 3–12 min; 5% A + 95% B for 12–14 min. The flowing rates were kept at 0.3 mL min<sup>-1</sup>. The injection volume was 5  $\mu\text{L}$ . The HPLC-separated components were coupled to the MS analyzer, and the MS detection was achieved by electrospray ionization (ESI) in the negative ion mode. The MS conditions were as follows: desolvation temperature, 400 °C; cone gas flow, 10 L h<sup>-1</sup>; desolvation gas flow, 800 L h<sup>-1</sup>; and cone voltage, 40 V.

### Browning of white mushroom

The absorption spectra of white mushroom surfaces were analyzed with UV-vis diffuse reflectance spectroscopy (UH4150, Hitachi, Tokyo, Japan) with BaSO<sub>4</sub> as a reflectance standard.

The intensity of reflection spectra was calculated by subtracting the initial spectra of mushroom slices without being immersed in flavonoid solutions from the spectra of samples immersed in flavonoid solutions at the time indicated.

The same-sized slices from the cap of white mushroom were soaked for 10 min in solutions of 100  $\mu\text{M}$  Api, Lut, Kaem and Quer in PBS buffer (5% DMSO), respectively, and dried out in the air followed by being adhered on glass slides. Changes in color and absorption spectra of the mushroom slices were recorded every hour by a camera and a diffuse reflectance spectrometer. A sample soaked only in PBS buffer was used in parallel as a control. All experiments were repeated three times, and the same tendency in browning promotion was observed.

## Abbreviations

TYR	Tyrosinase
Api	Apigenin
Lut	Luteolin
Kaem	Kaempferol
Quer	Quercetin
DMSO	Dimethyl sulfoxide
PBS	Phosphate buffer solution
DC	Dopachrome
DQ	Dopaoquinone
LP	Lag phase

## Funding

This work has been supported by grants from Natural Science Foundation of China (No. 22073114 and 21673288).

## Author contributions

Yao Lu: experiments, data processing and literature research. Yi Xu: guide in experimental procedures and problem discussion. Meng-Ting Song: diffuse reflectance spectroscopic experiment. Ling-Ling Qian: data analyses. Xiao-Lin Liu: provide suggestions in protein experiments. Rong-Yao Gao: instruction in fluorescence experiment. Rui-Min Han: the idea and completion of the project, manuscript writing. Leif H. Skibsted: problem discussion and language improvement. Jian-Ping Zhang: problem discussion and language improvement.

## Conflicts of interest

The authors declare no competing financial interest.

## References

- 1 Á. Sánchez-Ferrer, J. N. Rodríguez-López, F. García-Cánovas and F. García-Carmona, *Biochim. Biophys. Acta*, 1995, **1247**, 1–11.
- 2 T. Kobayashi, W. D. Vieira, B. Potterf, C. Sakai and G. Imokawa, *J. Cell Sci.*, 1995, **108**, 2301–2309.



3 P. A. Riley, *Int. J. Biochem. Cell Biol.*, 1997, **29**, 1235–1239.

4 C. Olivares, C. Jiménez-Cervantes, J. A. Lozano, F. Solano and J. C. García-Borrón, *Biochem. J.*, 2001, **354**, 131–139.

5 S.-Y. Seo, V. K. Sharma and A. N. Sharma, *J. Agric. Food Chem.*, 2003, **51**, 2837–2853.

6 S. Mondal, A. Thampi and M. Puranik, *J. Phys. Chem. B*, 2018, **122**, 2047–2063.

7 L. L. Baxter and W. J. Pavan, *Wiley Interdiscip. Rev.: Dev. Biol.*, 2013, **2**, 379–392.

8 F. Artés and M. C. M. I. Gil, *Food Sci. Technol. Int.*, 1998, **4**, 377–389.

9 J. P. Ebanks, R. R. Wickett and R. E. Boissy, *Int. J. Mol. Sci.*, 2009, **10**, 4066–4087.

10 H. Ando, M. S. Matsui and M. Ichihashi, *Int. J. Mol. Sci.*, 2010, **11**, 2566–2575.

11 M. E. Chiari, D. M. A. Vera, S. M. Palacios and M. C. Carpinella, *Bioorg. Med. Chem.*, 2011, **19**, 3474–3482.

12 M. Fan, G. Zhang, J. Pan and D. Gong, *Food Funct.*, 2017, **8**, 2601–2610.

13 S. Bolca, J. H. Li, D. Nikolic, N. Roche, P. Blondeel, S. Possemiers, D. De Keukeleire, M. Bracke, A. Heyerick, R. B. van Breemen and H. Depypere, *Mol. Nutr. Food Res.*, 2010, **54**, S284–S294.

14 L.-P. Xie, Q.-X. Chen, H. Huang, H.-Z. Wang and R.-Q. Zhang, *Biochemistry*, 2003, **68**, 487–491.

15 L.-C. Wu, L.-H. Chang, S.-H. Chen, N.-C. Fan and J.-A. Ho, *Food Sci. Technol. Int.*, 2009, **42**, 1513–1519.

16 H. X. Nguyen, N. T. Nguyen, M. H. K. Nguyen, T. H. Le, T. N. V. Do, T. M. Hung and M. T. T. Nguyen, *Chem. Cent. J.*, 2016, **10**, 2–6.

17 L. Zhang, X. Zhao, G.-J. Tao, J. Chen and Z.-P. Zheng, *Food Chem.*, 2017, **223**, 40–48.

18 D. Söhretoğlu, S. Sari, B. Barut and A. Öznel, *Bioorg. Chem.*, 2018, **81**, 168–174.

19 C. Shang, Y. Zhang, X. You, N. Guo, Y. Wang, Y. Fan and W. Liu, *Luminescence*, 2018, **33**, 681–691.

20 Y.-J. Kim and H. Uyama, *Cell. Mol. Life Sci.*, 2005, **62**, 1707–1723.

21 T.-S. Chang, *Int. J. Mol. Sci.*, 2009, **10**, 2440–2475.

22 M. R. Loizzo, R. Tundis and F. Menichini, *Compr. Rev. Food Sci. Food Saf.*, 2012, **11**, 378–398.

23 T.-S. Chang, *Materials*, 2012, **5**, 1661–1685.

24 T. Pillaiyar, V. Namasivayam, M. Manickam and S.-H. Jung, *J. Med. Chem.*, 2018, **61**, 7395–7418.

25 S. Zolghadri, A. Bahrami, M. T. H. Khan, J. Munoz-Munoz, F. Garcia-Molina, F. Garcia-Canovas and A. A. Saboury, *J. Enzyme Inhib. Med. Chem.*, 2019, **34**, 279–309.

26 M. Fan, H. Ding, G. Zhang, X. Hu and D. Gong, *LWT-Food Sci. Technol.*, 2019, **107**, 25–34.

27 B. Gąsowska-Bajger and H. Wojtasek, *J. Agric. Food Chem.*, 2016, **64**, 5417–5427.

28 A. Rescigno, F. Sollai, B. Pisu, A. Rinaldi and E. Sanjust, *J. Enzyme Inhib. Med. Chem.*, 2002, **17**, 207–218.

29 K. Bagherzadeh, F. S. Talari, A. Sharifi, M. R. Ganjali, A. A. Saboury and M. Amanlou, *J. Biomol. Struct. Dyn.*, 2015, **33**, 487–501.

30 Y.-L. Shi, I. F. F. Benzie and J. A. Buswell, *Life Sci.*, 2002, **70**, 1595–1608.

31 Y.-H. Hu, C.-M. Chen, L. Xu, Y. Cui, X.-Y. Yu, H.-J. Gao, Q. Wang, K. Liu, Y. Shi and Q.-X. Chen, *Postharvest Biol. Technol.*, 2015, **104**, 33–41.

32 B. Muszyńska, J. Piotrowska, A. Krakowska, A. Gruba, K. Kała, K. Sułkowska-Ziaja, A. Kryczyk and W. Opoka, *Eur. Food Res. Technol.*, 2017, **243**, 2135–2145.

33 M. Yan, B. Yuan, Y. Xie, S. Cheng, H. Huang and W. Zhang, *Postharvest Biol. Technol.*, 2020, **166**, 111230–111238.

34 S. Bi, L. Yan, Y. Wang, B. Pang and T. Wang, *J. Lumin.*, 2012, **132**, 2355–2360.

35 R. F. Steiner and I. Weinryb, *Excited States of Proteins and Nucleic Acids*, Plenum Press, New York, 1971, p. 40.

36 G. Zhang and Y. Ma, *Food Chem.*, 2013, **136**, 442–449.

37 Y. Q. Wang and H. M. Zhang, *J. Agric. Food Chem.*, 2013, **61**, 11191–11200.

38 J. Yang, Y. Xu, H.-Y. Liu, R.-M. Han, J.-P. Zhang and L. H. Skibsted, *Molecules*, 2017, **22**, 1757–1771.

39 Y. Xu, J. Yang, Y. Lu, L.-L. Qian, Z.-Y. Yang, R.-M. Han, J.-P. Zhang and L. H. Skibsted, *J. Phys. Chem. B*, 2020, **124**, 380–388.

40 L.-L. Qian, Y. Lu, Y. Xu, Z.-Y. Yang, Y.-M. Zhou, R.-M. Han, J.-P. Zhang and L. H. Skibsted, *RSC Adv.*, 2020, **10**, 30035–30047.

41 Z.-Y. Yang, L.-L. Qian, Y. Xu, M.-T. Song, C. Liu, R.-M. Han, J.-P. Zhang and L. H. Skibsted, *Molecules*, 2020, **25**, 1975–1987.

42 A. Andueza, A. García-Garzón, M. R. D. Galarreta, E. Ansorena, M. J. Iraburu, M. J. López-Zabalza and J. J. Martínez-Irujo, *Free Radical Biol. Med.*, 2015, **87**, 169–180.

43 M. Jiménez-Atiénzar, J. Escribano, J. Cabanes, F. Gandía-Herrero and F. García-Carmona, *Plant Physiol. Biochem.*, 2005, **43**, 866–873.

44 K. Amaki, E. Saito, K. Taniguchi, K. Joshita and M. Murata, *Biosci., Biotechnol., Biochem.*, 2011, **75**, 829–832.

45 A. Narai-Kanayama, Y. Uekusa, F. Kiuchi and T. Nakayama, *J. Agric. Food Chem.*, 2018, **66**, 13464–13472.

46 M. J. Waterman, A. S. Nugraha, R. Hendra, G. E. Ball, S. A. Robinson and P. A. Keller, *J. Nat. Prod.*, 2017, **80**, 2224–2231.

47 Y. Oztekin, Z. Yazicigil, A. Ramanaviciene and A. Ramanavicius, *Sens. Actuators, B*, 2011, **152**, 37–48.

48 M. Fan, G. Zhang, X. Hu, X. Xu and D. Gong, *Food Res. Int.*, 2017, **100**, 226–233.

49 Z. Xiong, W. Liu, L. Zhou and J. Chen, *Food Chem.*, 2016, **203**, 430–439.

50 A. M. Pannala, T. S. Chan, P. J. O'Brien and C. A. Rice-Evans, *Biochem. Biophys. Res. Commun.*, 2001, **282**, 1161–1168.

51 Y. Xu, A. H. Stokes, W. M. Freeman, S. C. Kumer, B. A. Vogt and K. E. Vrana, *Mol. Brain Res.*, 1997, **45**, 159–162.

